Mathematical Biosciences and Engineering

http://www.aimspress.com/journal/mbe

MBE, 19(12): 11854–11867.
DOI: 10.3934/mbe.2022553
Received: 01 June 2022
Revised: 24 July 2022
Accepted: 02 August 2022
Published: 17 August 2022

Research article

Turing pattern induced by the directed ER network and delay

Qianqian Zheng[1], Jianwei Shen[2,*], Lingli Zhou[3] and Linan Guan[2]

[1] School of Science, Xuchang University; Henan Joint International Research Laboratory of High Performance Computation for Complex Systems, Xuchang 461000, China

[2] School of Mathematics and Statistics, North China University of Water Resources and Electric Power, Zhengzhou 450046, China

[3] School of Mathematical Sciences, Soochow University, Suzhou 215006, China

* **Correspondence:** Email: xcjwshen@gmail.com.

Abstract: Infectious diseases generally spread along with the asymmetry of social network propagation because the asymmetry of urban development and the prevention strategies often affect the direction of the movement. But the spreading mechanism of the epidemic remains to explore in the directed network. In this paper, the main effect of the directed network and delay on the dynamic behaviors of the epidemic is investigated. The algebraic expressions of Turing instability are given to show the role of the directed network in the spread of the epidemic, which overcomes the drawback that undirected networks cannot lead to the outbreaks of infectious diseases. Then, Hopf bifurcation is analyzed to illustrate the dynamic mechanism of the periodic outbreak, which is consistent with the transmission of COVID-19. Also, the discrepancy ratio between the imported and the exported is proposed to explain the importance of quarantine policies and the spread mechanism. Finally, the theoretical results are verified by numerical simulation.

Keywords: SIR; pattern formation; network; turing instability; delay

1. Introduction

Pattern formation is a kind of spatial dynamical behavior that shows species distribution and is widely used to explain some biological mechanisms [1–6]. With the development of complex networks, more and more attention is paid to pattern formation from the perspective of complex networks [7]. Turing instability was investigated to show the effect of the network on the pattern formation [8], which is different from the reaction-diffusion system. Then, the theory of pattern formation was proposed through the distribution of the real and imaginary parts of the eigenvalues on directed networks [9]. The instability mechanism on network was explored by comparing the instability region in the reaction-

diffusion and network-organized system [10,11]. Meanwhile, the concept of negative wavenumber was introduced to explain the interactions between network nodes [12], which was also used to illustrate the dynamic behaviors of the epidemic [13]. Although some work about Turing instability and pattern formation has been done on directed networks [14], the function of delay in the epidemic model with the directed network remains to be explored.

The mathematical model is a vital tool to describe the spreading of infectious diseases [15–18] and is used to explain the dynamic behaviors of COVID-19 [19–24]. The SIRS model is a classic model to describe the spreading of infectious diseases and has been extended to many infectious disease models [25, 26]. The bifurcation of an SIRS model with a nonlinear incidence rate was analyzed to make strategies for controlling the epidemic [27]. And then the corresponding SDE version of the SIRS model was developed to show the effect of the basic reproduction number on the dynamical behavior and the prevalence of the epidemic [28]. The SIRS model with both noise and delay [29, 30] was analyzed to help the government control the spreading of infectious diseases further. Recently, the study of infectious diseases with social networks was presented to capture the periodic outbreak behaviors of infectious diseases [31, 32]. But because infectious diseases generally spread along with the directed network (social network) propagation, the SIRS model with the directed network should be considered.

Although infectious diseases generally spread along with social networks, the isolation policy also leads to the direction of propagation(the asymmetry of network propagation). Meanwhile, there is also a time delay in the propagation process of the epidemic. To understand the spread mechanism and spatiotemporal dynamic behavior of the epidemic in the directed network, pattern formation in the epidemic model with the directed network is investigated to show the effect of the directed network and delay on the outbreak of the epidemic. Firstly, we analyze a general system with the directed network and obtain the conditions of Turing instability. Then, we illustrate the effect of the directed network and delay on the Hopf bifurcation. Also, the dynamical mechanism of the epidemic model with network and delay is explained. According to our theories, some epidemic prevention strategies are given. Finally, numerical simulation verifies our results.

2. Model description

The goal of this paper is to study the following network-organized system

$$\begin{aligned} \frac{dS_i}{dt} &= f(S_i, I_i, S_i(t-\tau), I_i(t-\tau)) + d_1 \sum_{k=1}^{n} A_{ik}^{(1)} h_1(S_k, S_i), \\ \frac{dI_i}{dt} &= g(S_i, I_i, S_i(t-\tau), I_i(t-\tau)) + d_2 \sum_{k=1}^{n} A_{ik}^{(2)} h_2(I_k, I_i), \end{aligned} \tag{2.1}$$

where $f(S, I, S(t-\tau), I(t-\tau))$, $g(S, I, S(t-\tau), I(t-\tau))$ are the interactions between species, $A^{(1)}, A^{(2)}$ are the adjacent matrix of the directed networks, $h_1(S_k, S_i), h_2(I_k, I_i)$ are the interaction functions through network, and the specific example can be found in Results and discussion. Also, we assume system (2.1) is stable when $d_1 = d_2 = 0$.

The linear network-organized system without delay can be expressed as

$$\begin{aligned} \frac{dS_i}{dt} &= a_{11}S_i + a_{12}I_i + d_1 \sum_{k=1}^{n} L_{ik}^{(1)} S_k, \\ \frac{dI_i}{dt} &= a_{21}S_i + a_{22}I_i + d_2 \sum_{k=1}^{n} L_{ik}^{(2)} I_k, \end{aligned} \tag{2.2}$$

where $a_{11}, a_{12}, a_{21}, a_{22}$ are the linear parts of $f(S_i, I_i, S_i(t-\tau), I_i(t-\tau)), g(S_i, I_i, S_i(t-\tau), I_i(t-\tau))$ at equilibrium point when $\tau = 0$, $L_{ik}^{(1)} S_k, L_{ik}^{(2)} I_k$ are the linear parts of $A_{ik}^{(1)} h_1(S_k, S_i), A_{ik}^{(2)} h_2 h(S_k, S_i)$. In general, $L^{(1)}, L^{(2)}$ are the Laplacian matrices and generally have the same eigenvectors.

The eigenvalues and the eigenvectors of matrices $L^{(1)}, L^{(2)}$ can be defined [9]

$$\begin{aligned} \sum_{k=1}^{n} L_{ik}^{(1)} v_k^m &= (\theta_m + \Theta_m j) v_i^m, \\ \sum_{k=1}^{n} L_{ik}^{(2)} v_k^m &= (\phi_m + \Phi_m j) v_i^m, \end{aligned}$$

where same eigenvector space is true for $L^{(1)}, L^{(2)}$.

The general solution of the linear network-organized system can be expanded as

$$S_i = \sum_{k=1}^{n} c_k e^{\lambda_k t} v_i^k, I_i = \sum_{k=1}^{n} b_k e^{\lambda_k t} v_i^k, \tag{2.3}$$

where λ represents λ_k for convenience in the following.

Substituting system (2.3) into system (2.2), one has the Jacobian matrix

$$J_0 = \begin{pmatrix} \lambda - a_{11} - d_1(\theta_i + \Theta_i j) & -a_{12} \\ -a_{21} & \lambda - a_{22} - d_2(\phi_i + \Phi_i j) \end{pmatrix},$$

where θ_i, ϕ_i and Θ_i, Φ_i are the real parts and the imaginary parts of Λ_i^1, Λ_i^2, separately. $j(j^2 = -1)$ is the imaginary part unit.

According to the Jacobian matrix, we have the characteristic equation

$$\lambda^2 + (c_1 + c_2 j)\lambda + c_3 + c_4 j = 0, \tag{2.4}$$

where

$$\begin{aligned} c_1 &= -a_{11} - d_1\theta_i - a_{22} - d_2\phi_i, \\ c_2 &= -d_2\Phi_i - d_1\Theta_i, \\ c_3 &= -d_1\Theta_i d_2\Phi_i - a_{12}a_{21} + a_{11}a_{22} + a_{11}d_2\phi_i + d_1\theta_i a_{22} + d_1\theta_i d_2\phi_i, \\ c_4 &= a_{11}d_2\Phi_i + d_1\Theta_i d_2\phi_i + d_1\Theta_i a_{22} + d_1\theta_i d_2\Phi_i. \end{aligned}$$

The roots of system (2.4) are

$$\lambda_{1,2} = \frac{-c_1 - jc_2 \pm \sqrt{(c_1 + jc_2)^2 - 4\,c_3 - 4\,jc_4}}{2}.$$

Before we consider the sign of the $\lambda_{1,2}$, a complex number $z = a + bj$ can be defined as

$$\sqrt{z} = \pm\left(\sqrt{\frac{a+|z|}{2}} + sgn(b)\sqrt{\frac{-a+|z|}{2}}\, j\right),$$

where $sgn(.)$ is the standard sign function, $a = {c_1}^2 - {c_2}^2 - 4\,c_3$, $b = 2\,c_1c_2 - 4\,c_4$, and

$$\lambda_{1,2} = \frac{-c_1 - jc_2 \pm (\sqrt{\frac{a+|z|}{2}} + sgn(b)\sqrt{\frac{-a+|z|}{2}}\,j)}{2}.$$

To investigate the stability of system (2.1), the sign of the maximum real part of $\lambda_{1,2}$ is

$$s_1 = -c_1 + \sqrt{\frac{a+|z|}{2}} = -c_1 + \sqrt{\frac{a+\sqrt{a^2+b^2}}{2}} > 0. \tag{2.5}$$

Namely, system (2.1) is unstable when H_1 holds ($s_1 > 0$), where

$$H_1: \quad c_1 = -a_{11} - d_1\theta_i - a_{22} - d_2\phi_i \le 0.$$

If H_1 is not true,

$$c_1 = -a_{11} - d_1\theta_i - a_{22} - d_2\phi_i > 0,$$

and system (2.5) can be rewritten as

$$\sqrt{\frac{a+\sqrt{a^2+b^2}}{2}} > c_1.$$

Then, one has the following inequality

$$\begin{aligned} &s_2 = -{c_1}^2 - {c_2}^2 - 4\,c_3 \\ &+ \sqrt{{c_1}^4 + 2\,{c_1}^2{c_2}^2 - 8\,{c_1}^2c_3 + {c_2}^4 + 8\,{c_2}^2c_3 + 16\,{c_3}^2 - 16\,c_1c_2c_4 + 16\,{c_4}^2} \\ &> 0, \end{aligned} \tag{2.6}$$

It is found that system (2.1) is unstable ($s_2 > 0$) when H_2 holds, where

$$H_2: \quad -{c_1}^2 - {c_2}^2 - 4\,c_3 > 0.$$

If H_2 is not true,

$$-{c_1}^2 - {c_2}^2 - 4\,c_3 < 0,$$

system (2.6) can be expressed as

$$\begin{aligned} &\sqrt{{c_1}^4 + 2\,{c_1}^2{c_2}^2 - 8\,{c_1}^2c_3 + {c_2}^4 + 8\,{c_2}^2c_3 + 16\,{c_3}^2 - 16\,c_1c_2c_4 + 16\,{c_4}^2} \\ &> {c_1}^2 + {c_2}^2 + 4\,c_3 \end{aligned}$$

and it is equivalent to

$$H_3: \quad s_3 = -{c_1}^2c_3 - c_1c_2c_4 + {c_4}^2 > 0.$$

If H_3 holds, Turing instability and Hopf bifurcation may occur. Assume $\lambda = j\omega$, system (2.4) can be written as

$$-\omega^2 + (c_1\,j - c_2)\omega + c_3 + c_4\,j = 0. \tag{2.7}$$

If a positive real root ω_0 of system (2.7) and the transversality condition $Re(\frac{d\lambda}{d\mu})_{\omega=\omega_0,\mu=\mu_c} \neq 0$($\mu$ is a parameter and its critical value μ_c) hold [33], Hopf bifurcation occurs.

Assume system (2.1)is stable when $d_1 = d_2 = 0$. Then, the network-organized system with delay is considered, and the linear parts of system (2.1) can be expressed as

$$\begin{aligned} \frac{dS_i}{dt} &= b_{11}S_i + b_{12}I_i + b_{13}S_i(t-\tau) + b_{14}I_i(t-\tau) + d_1\sum_{k=1}^{n} L_{ik}S_k, \\ \frac{dI_i}{dt} &= b_{21}S_i + b_{22}I_i + b_{23}S_i(t-\tau) + b_{24}I_i(t-\tau) + d_2\sum_{k=1}^{n} L_{ik}I_k, \end{aligned} \tag{2.8}$$

where $b_{11}, b_{12}, b_{13}, b_{14}, b_{21}, b_{22}, b_{23}, b_{24}$ are the linear parts of $f(S_i, I_i, S_i(t-\tau), I_i(t-\tau)), g(S_i, I_i, S_i(t-\tau), I_i(t-\tau))$ at equilibrium point.

Substituting system (2.3) into system (2.8), one has the Jacobian matrix

$$J = \begin{pmatrix} \lambda - b_{11} - b_{13}e^{-\lambda\tau} - d_1(\theta_i + \Theta_i j) & -b_{12} - b_{14}e^{-\lambda\tau} \\ -b_{21} - b_{23}e^{-\lambda\tau} & \lambda - b_{22} - b_{24}e^{-\lambda\tau} - d_2(\phi_i + \Phi_i j) \end{pmatrix}$$

and the characteristic equation is

$$\lambda^2 + (c_{11}e^{-\lambda\tau} + c_{12} + c_{13}j)\lambda + (c_{14} + c_{15}j)e^{-\lambda\tau} + c_{16} + c_{17}j = 0, \tag{2.9}$$

where

$$\begin{aligned}
c_{11} &= -b_{13} - b_{24}, \\
c_{12} &= -d_2\,\phi_i - \theta_i\,d_1 - b_{11} - b_{22}, \\
c_{13} &= -d_2\,\Phi_i - \Theta_i\,d_1, \\
c_{14} &= b_{13}\,d_2\,\phi_i + b_{24}\,\theta_i\,d_1 - b_{23}\,\mathtt{b}_{12} + b_{11}\,b_{24} + b_{13}\,b_{22} - b_{14}\,b_{21}, \\
c_{15} &= b_{13}\,d_2\,\Phi_i + b_{24}\,\Theta_i\,d_1, \\
c_{16} &= -d_2\,\Phi_i\,\Theta_i\,d_1 + d_2\,\phi_i\,\theta_i\,d_1 + b_{11}\,d_2\,\phi_i + b_{22}\,\theta_i\,d_1 - b_{21}\,\mathtt{b}_{12} + b_{11}\,b_{22}, \\
c_{17} &= d_2\,\Phi_i\,\theta_i\,d_1 + d_2\,\Theta_i\,\phi_i\,d_1 + b_{11}\,d_2\,\Phi_i + b_{22}\,\Theta_i\,d_1.
\end{aligned}$$

To investigate the Hopf bifurcation of system (2.9), we substitute $\lambda = j\omega$ into system (2.9), and have

$$\begin{aligned}
&-\omega^2 + \omega\,c_{11}\sin(\omega\,\tau) - \omega\,c_{13} + \cos(\omega\,\tau)\,c_{14} + \sin(\omega\,\tau)\,c_{15} + c_{16} \\
&+j\,(\omega\,c_{11}\cos(\omega\,\tau) + \omega\,c_{12} - \sin(\omega\,\tau)\,c_{14} + \cos(\omega\,\tau)\,c_{15} + c_{17}) = 0.
\end{aligned} \tag{2.10}$$

Separating the real and imaginary parts of system (2.10), one has

$$\begin{aligned}
&-\omega^2 + \omega\,c_{11}\sin(\omega\,\tau) - \omega\,c_{13} + \cos(\omega\,\tau)\,c_{14} + \sin(\omega\,\tau)\,c_{15} + c_{16} = 0, \\
&\omega\,c_{11}\cos(\omega\,\tau) + \omega\,c_{12} - \sin(\omega\,\tau)\,c_{14} + \cos(\omega\,\tau)\,c_{15} + c_{17} = 0.
\end{aligned} \tag{2.11}$$

and the solutions are

$$\begin{aligned}
\cos(\omega\,\tau) &= -\tfrac{\omega^2 c_{11}c_{12} - \omega^2 c_{14} + \omega\,c_{11}c_{17} + \omega\,c_{12}c_{15} - \omega\,c_{13}c_{14} + c_{14}c_{16} + c_{15}c_{17}}{\omega^2 {c_{11}}^2 + 2\,\omega\,c_{11}c_{15} + {c_{14}}^2 + {c_{15}}^2}, \\
\sin(\omega\,\tau) &= \tfrac{\omega^3 c_{11} + \omega^2 c_{11}c_{13} + \omega^2 c_{15} - \omega\,c_{11}c_{16} + \omega\,c_{12}c_{14} + \omega\,c_{13}c_{15} + c_{14}c_{17} - c_{15}c_{16}}{\omega^2 {c_{11}}^2 + 2\,\omega\,c_{11}c_{15} + {c_{14}}^2 + {c_{15}}^2}.
\end{aligned} \tag{2.12}$$

According to $\cos^2(\omega\,\tau) + \sin^2(\omega\,\tau) = 1$, we have

$$p_0\omega^6 + p_1\omega^5 + p_2\omega^4 + p_3\omega^3 + p_4\omega^2 + p_5\omega + p_6 = 0, \tag{2.13}$$

where

$$\begin{aligned}
p_0 &= {c_{11}}^2, \\
p_1 &= 2\,{c_{11}}^2 c_{13} + 2\,c_{11}c_{15}, \\
p_2 &= -{c_{11}}^4 + {c_{11}}^2{c_{12}}^2 + {c_{11}}^2{c_{13}}^2 - 2\,{c_{11}}^2 c_{16} + 4\,c_{11}c_{13}c_{15} + {c_{14}}^2 + {c_{15}}^2, \\
p_3 &= -4\,{c_{11}}^3 c_{15} + 2\,{c_{11}}^2 c_{12}c_{17} - 2\,{c_{11}}^2 c_{13}c_{16} + 2\,c_{11}{c_{12}}^2 c_{15} + 2\,c_{11}{c_{13}}^2 c_{15} \\
&-4\,c_{11}c_{15}c_{16} + 2\,c_{13}{c_{14}}^2 + 2\,c_{13}{c_{15}}^2, \\
p_4 &= -2\,{c_{11}}^2{c_{14}}^2 - 6\,{c_{11}}^2{c_{15}}^2 + {c_{11}}^2{c_{16}}^2 + {c_{11}}^2{c_{17}}^2 + 4\,c_{12}c_{15}c_{17}c_{11} \\
&-4\,c_{11}c_{13}c_{15}c_{16} + {c_{12}}^2{c_{14}}^2 + {c_{12}}^2{c_{15}}^2 + {c_{13}}^2{c_{14}}^2 + {c_{13}}^2{c_{15}}^2 - 2\,{c_{14}}^2 c_{16} - 2\,{c_{15}}^2 c_{16}, \\
p_5 &= -4\,c_{11}{c_{14}}^2 c_{15} - 4\,c_{11}{c_{15}}^3 + 2\,c_{11}c_{15}{c_{16}}^2 + 2\,c_{11}c_{15}{c_{17}}^2 + 2\,c_{12}{c_{14}}^2 c_{17} \\
&+2\,c_{12}{c_{15}}^2 c_{17} - 2\,c_{13}{c_{14}}^2 c_{16} - 2\,c_{13}{c_{15}}^2 c_{16}, \\
p_6 &= -{c_{14}}^4 - 2\,{c_{14}}^2{c_{15}}^2 + {c_{14}}^2{c_{16}}^2 + {c_{14}}^2{c_{17}}^2 - {c_{15}}^4 + {c_{15}}^2{c_{16}}^2 + {c_{15}}^2{c_{17}}^2.
\end{aligned}$$

Based on Hurwitz criterion [33], if H_4 holds, system (2.2) is always stable, otherwise Turing instability induced by network occurs .

$$H_4: \quad \begin{array}{l} p_i > 0 (i = 0, ..., 6), \\ D_n > 0 (n = 1, ..., 6), \end{array}$$

where

$$D_n = \begin{vmatrix} p_1 & p_0 & 0 & 0 & 0 & 0 \\ p_3 & p_2 & p_1 & 0 & 0 & 0 \\ p_5 & p_4 & p_3 & p_2 & p_1 & p_0 \\ 0 & p_6 & p_5 & p_4 & p_3 & p_2 \\ 0 & 0 & 0 & p_6 & p_5 & p_4 \\ 0 & 0 & 0 & 0 & 0 & p_6 \end{vmatrix}$$

If $s(1 \le s \le 6)$ positive real roots $\omega_i (1 \le i \le s)$ exist in system (2.13), Hopf bifurcation occurs. And the critical value τ_c can be obtained from system (2.14),

$$\tau_c = min_{1 \le i \le s} \{ \frac{1}{\omega_i} \arccos(-\frac{Q_1}{Q_2}) \}, \tag{2.14}$$

where $Q_1 = \omega_i{}^2 c_{11} c_{12} - \omega_i{}^2 c_{14} + \omega_i c_{11} c_{17} + \omega_i c_{12} c_{15} - \omega_i c_{13} c_{14} + c_{14} c_{16} + c_{15} c_{17}$, $Q_2 = \omega_i{}^2 c_{11}{}^2 + 2\,\omega_i c_{11} c_{15} + c_{14}{}^2 + c_{15}{}^2$, and τ_0 is the critical value of τ_c without network, τ_1 is the critical value of τ_c with network. Also, the transversality condition $Re(\frac{d\lambda}{d\tau}) \ne 0$ [34, 35].

Theorem 1 In the network-organized system, If one of H_1, H_2, H_3 and the transversality condition $Re(\frac{d\lambda}{d\tau}) > 0$ hold, Turing instability induced by network occurs; if H_4 does not hold, Turing instability induced by network may occur when $\tau_0 > \tau_1$ and $\tau_0 > \tau > \tau_1$.

Proof: It is well known that system (2.1) without network is stable when $\tau < \tau_0$. And the network could induce the decrease of τ_c to τ_1. Namely, system (2.1) is unstable when $\tau > \tau_1$. As a result, $\tau_0 > \tau > \tau_1$ means Turing instability occurs.

3. Results and discussion

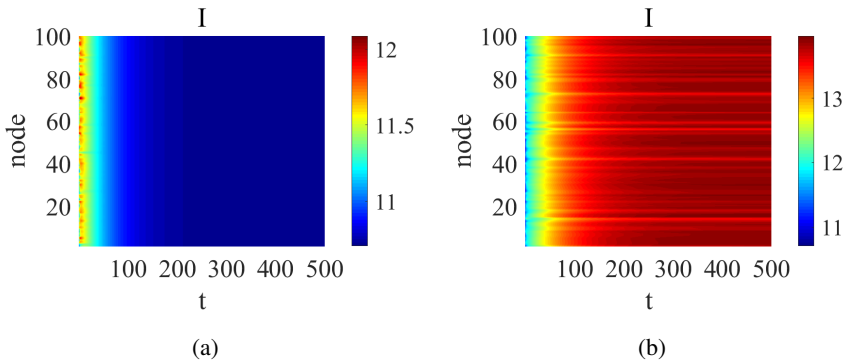

Figure 1. The stability of the system (2.4) when $\alpha = 0.2, \beta = 1/14, \gamma = 0.01, \delta = 0.1, d = 1/60, d_1 = 0.1, d_2 = 0.1, p = 0.05, \tau = 0$. (a) The equilibrium point E_1 is stable when $q = 1$. (b) Turing instability occurs when $q = 0.99$.

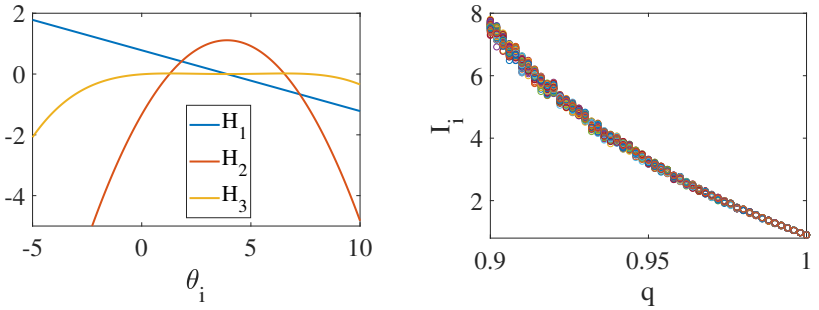

(a) (b)

Figure 2. The bifurcation of the system (2.4) when $\alpha = 0.2, \beta = 1/14, \gamma = 0.01, \delta = 0.1, d = 1/60, d_1 = 0.1, d_2 = 0.1, p = 0.05, \tau = 0$. (a) Turing instability region about θ_i. (b) The distribution of the infected in different nodes about q.

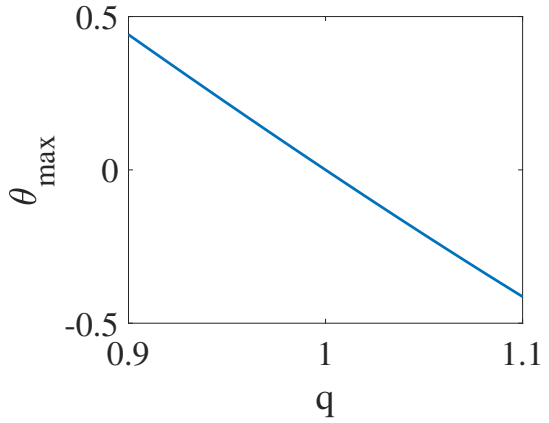

Figure 3. The maximum θ_{max} of θ_i about q when $\alpha = 0.2, \beta = 1/14, \gamma = 0.01, \delta = 0.1, d = 1/60, d_1 = 0.1, d_2 = 0.1, p = 0.05, \tau = 0$.

In this section, we take an SIRS model as an example to illustrate our theoretical results through numerical simulation. A general SIRS model can be written as

$$\begin{aligned} \frac{dS}{dt} &= \alpha - \beta S(t-\tau)I(t-\tau) - dS + \delta R, \\ \frac{dI}{dt} &= \beta S(t-\tau)I(t-\tau) - \gamma I - dI, \\ \frac{dR}{dt} &= \gamma I - \delta R - dR. \end{aligned}$$

Assume $\frac{dR}{dt} = 0$, one has the following system,

$$\begin{aligned} \frac{dS}{dt} &= \alpha - \beta S(t-\tau)I(t-\tau) - dS + \frac{\delta\gamma}{d+\delta} I, \\ \frac{dI}{dt} &= \beta S(t-\tau)I(t-\tau) - dI - \gamma I, \end{aligned}$$

where the equilibrium point (S^*, I^*) is $E_1 = (\frac{\alpha}{d}, 0)$, $E_2 = (\frac{d+\gamma}{\beta}, -\frac{-\alpha d\beta - \alpha\delta\beta + d^3 + d^2\delta + d^2\gamma + d\delta\gamma}{\beta d(\gamma+d+\delta)})$.

In this paper, we consider the network-organized system

$$\begin{aligned} \frac{dS_i}{dt} &= \alpha - \beta S_i(t-\tau)I_i(t-\tau) - dS_i + \frac{\delta\gamma}{d+\delta} I_i + d_1 \sum_{k=1}^{n} A_{ik} f(S_k, S_i), \\ \frac{dI_i}{dt} &= \beta S_i(t-\tau)I_i(t-\tau) - dI_i - \gamma I_i + d_2 \sum_{k=1}^{n} A_{ik} g(I_k, L_i), \end{aligned} \tag{3.1}$$

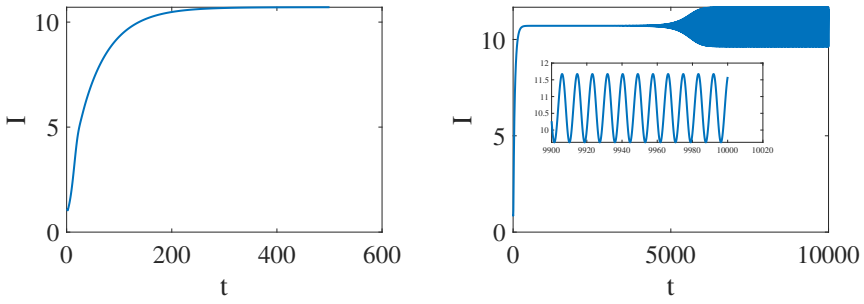

Figure 4. The stability of the system (2.4) when $\alpha = 0.2, \beta = 1/14, \gamma = 0.01, \delta = 0.1, d = 1/60, d_1 = 0, d_2 = 0$. (a) The equilibrium point E_1 is stable when $\tau = 2.17 < \tau_0 = 2.175$. (b) The periodic oscillation state occurs when $\tau = 2.18 > \tau_0 = 2.175$.

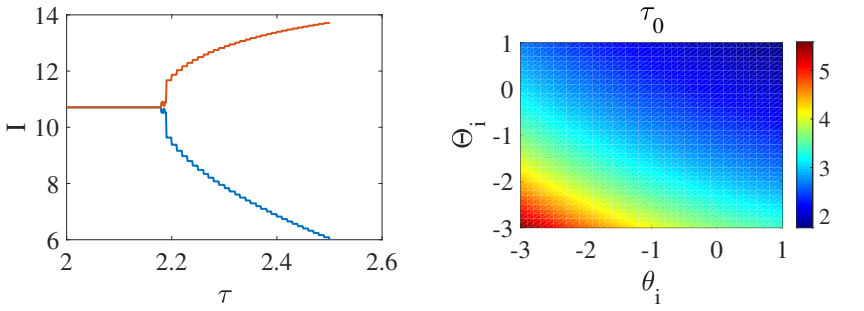

Figure 5. The stability of the system (2.4) when $\alpha = 0.2, \beta = 1/14, \gamma = 0.01, \delta = 0.1, d = 1/60, d_1 = 0.1, d_2 = 0.1$. (a) The bifurcation about τ of the system(2.4) without network. (b) The distribution of τ_0 about θ_i, Θ_i.

Suppose $f(S_k, S_i) = S_j - qS_i, g(I_k, L_i) = I_j - qI_i$, we obtain

$$\frac{dS_i}{dt} = \alpha - \beta S_i(t-\tau)I_i(t-\tau) - dS_i + \frac{\delta\gamma}{d+\delta}I_i + d_1\sum_{k=1}^{n} A_{ik}(S_j - qS_i),$$
$$\frac{dI_i}{dt} = \beta S_i(t-\tau)I_i(t-\tau) - dI_i - \gamma I_i + d_2\sum_{k=1}^{n} A_{ik}(I_j - qI_i),$$

where $\alpha = 0.2, \beta = 1/14, \gamma = 0.01, \delta = 0.1, d = 1/60$; q is the discrepancy ratio between the imported and the exported, $q = 1$ means the imported equal to the exported, $q > 1$ means the imported is smaller than the exported, $q < 1$ means the imported is larger than the exported.

We firstly consider the system (2.1) without delay. Based on Theorem 1, Turing instability never occur when $q = 1$ (the imported equals to the exported) (Figure 1(a)). Namely, the diffusion (network) of the infected(the susceptible) does not work in the outbreak, which does not match the reality [13, 31]. And H_1, H_2, H_3 hold if $q = 0.99$, the directed network leads to Turing instability (Figure 1(b)). Therefore, the discrepancy ratio is vital for the spread of the epidemic (Figure 2). That's why the importation of cases is strictly controlled in some countries. From Figure 2, one of H_1, H_2, H_3 may hold if a θ_i exists (Figure 2(a)). Meanwhile, the outbreak intensity and maximum $\theta_{max}(\theta_{max}$ is the

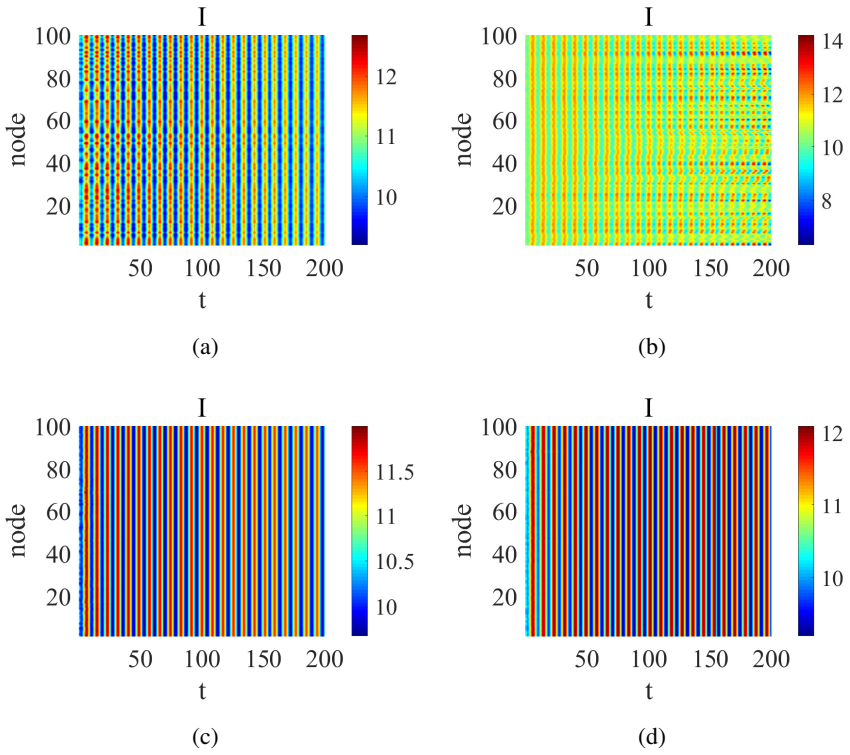

Figure 6. The stability of the system (2.4) when $\alpha = 0.2, \beta = 1/14, \gamma = 0.01, \delta = 0.1, d = 1/60$. (a) Turing instability occurs when $\tau = 2.17, p = 0.1, d_1 = 0.1, d_2 = 0$. (b) Turing stability occurs when $\tau = 2.17, p = 0.1, d_1 = 0, d_2 = 0.1$. (c) Turing instability occurs when $\tau = 2.17, p = 0.1, d_1 = 0.1, d_2 = 0.1$. (d) Turing instability occurs when $\tau = 2.2, p = 0.1, d_1 = 0.1, d_2 = 0.1$.

maximum real part of θ_i) decreases with the increase of q (Figure 2(b), Figure 3). Namely, q is a key factor in instability (Figures 2 and 3). Namely, controlling the imported cases is a good way to reduce the outbreaks of infectious diseases. Also, the directed network is more suitable than the undirected network to explain the transmission mechanism of infectious diseases because the undirected network doesn't work in some models [13, 31].

Then, we consider the system (2.1). Supposing the incubation period is a time delay, the delay could affect the stability of system (2.1) and make the periodic oscillation state occur when $\tau = 2.18 > \tau_0 = 2.175$ (Figure 4). Also, the outbreak intensity is in direct proportion to τ (Figure 5(a)) and τ_0 is inversely proportional to θ_i, Θ_i[Figure 5(b)]. From Figure 5(b), Θ_i and θ_i could lead to the decrease of τ_c and Turing instability in the directed network-organized system. From Figure 4, system (2.1) without network is stable when $\tau = 2.17$, but Turing instability occurs in system (2.1) when $\tau = 2.17$ because the critical τ_c decreases to τ_1 and $\tau_0 > \tau > \tau_1$(Figure 6). Furthermore, the diffusion(on network) of the susceptible (Figure 6(a))(or the infected[Figure 6(b)]) alone leads to instability. Of course, the diffusion of the infected bring about the larger outbreak (Figure 6(a),(b)). It is found that the diffusion of the susceptible and infected could make outbreaks of the epidemic more synchronous (Figure 6(c)). So is Figure 6(c) when τ is larger than τ_0. Finally, we investigate the effect of the discrepancy ratio q on the pattern formation of system (2.1) (Figures 7 and 8). If $p = 0.01$ is small, system (2.1) is stable (Figure

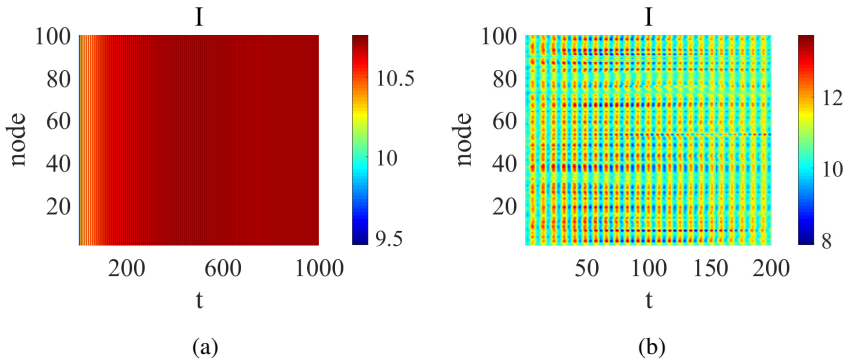

Figure 7. The stability of the system (2.4) when $\alpha = 0.2, \beta = 1/14, \gamma = 0.01, \delta = 0.1, d = 1/60, d_1 = 0.1, d_2 = 0.1, p = 0.01$. (a) The stability of the system(2.4) is stable when $q = 1, p = 0.01$. (b) Turing instability occurs when $q = 0.99, p = 0.01$.

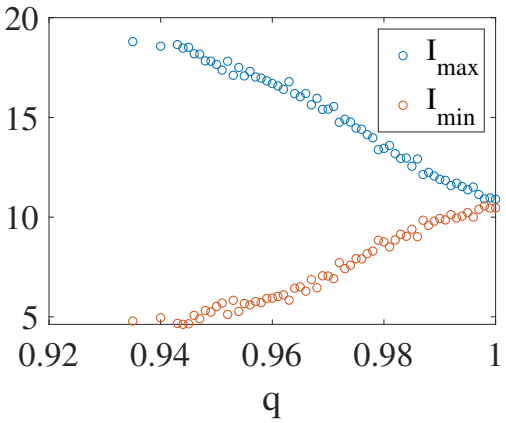

Figure 8. The maximum/minimum of I_i about q when $\alpha = 0.2, \beta = 1/14, \gamma = 0.01, \delta = 0.1, d = 1/60, d_1 = 0.1, d_2 = 0.1, p = 0.01, \tau = 2.17$.

7(a)), and Turing instability occurs when $q = 0.99, p = 0.01$ (Figure 7(a)). Also, the discrepancy ratio q could make the regional differences even greater (Figure 7). Although the maximum I_{max} is reduced, the minimum I_{min} is increasing, it ultimately becomes more uniform (Figure 7). Finally, the numerical results qualitatively agree with the periodic outbreaks and distribution of COVID-19 (Figure 9).

Through the above analysis, it is found that the discrepancy ratio q and time delay τ play a vital role in the outbreak of the epidemic. And controlling the imported cases is a good way to reduce the outbreaks of infectious diseases, which could increase the discrepancy ratio. Because the incubation period τ_0 is the inherent nature of infectious diseases, it is impossible to change. But we can control the region of τ_1 through the directed network, which also provides a novel to prevent the epidemic.

4. Conclusions

In this paper, the effect of the directed network and delay on the spread of the epidemic is investigated, which overcome the shortage of the undirected network (The undirected network can't lead to the outbreak of infectious diseases in some model [13, 31]). The conditions of Turing instability

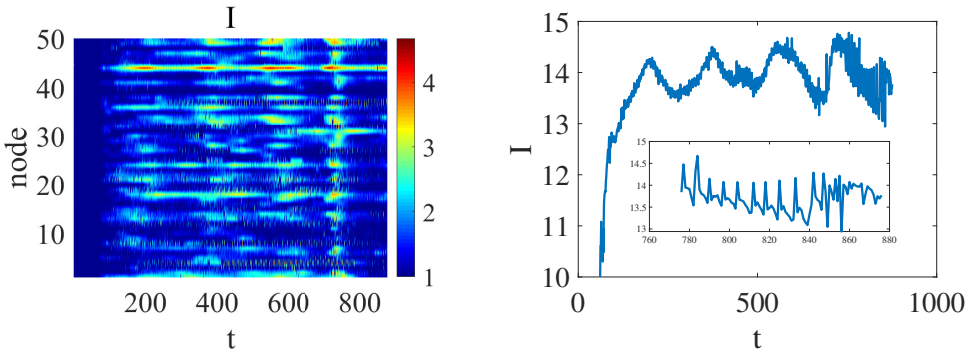

Figure 9. The new confirmed cases of COVID-19 from Jan, 2020 to May, 2022 in Africa (https://covid19.who.int/data). (a) The new confirmed cases ($log_{10}(I)$) of 50 countries in Africa. (b) The new confirmed cases($log_{10}(I)$) in Africa.

are given in a general system with the directed network, which is an important indicator to determine whether an outbreak occurs. Then, Hopf bifurcation is analyzed to illustrate the role of the delay and directed network in Turing instability, which can be controlled through the directed network. Also, the proposed discrepancy ratio could make the regional differences even more significant[Figure.9(a)], which is an essential indicator in assessing quarantine policies. Finally, although the combination of the directed network and delay may be a novel way to investigate the pattern dynamics, the general interaction function through the network is difficult to express in the stability of a network-organized system, which will be further studied.

Acknowledgments

This work is supported by National Natural Science Foundation of China (12002297), Basic research Project of Universities in Henan Province (21zx009), Program for Science& Technology Innovation Talents in Universities of Henan Province (22HASTIT018), The Scientific Research Innovation Team of Xuchang University (2022CXTD002), Outstanding Young Backbone Teacher of Xuchang University (2022), Key scientific research projects of Henan Institutions of Higher learning in 2021 (21B130004).

Conflict of interest

The authors declare there is no conflict of interest.

References

1. A. M. Turing , The chemical basis of morphogenesis, *Bull. Math. Biol.*, **52** (1990), 153–197. https://doi.org/10.1007/BF02459572
2. P. K. Maini, R. E. Baker, C. M. Chuong, The Turing model comes of molecular age, *Science*, **314** (2006), 1397–1398. https://www.science.org/doi/10.1126/science.1136396

3. Q. Zheng, J. Shen, Z. Wang, Pattern formation and oscillations in reaction-diffusion model with p53-Mdm2 feedback loop, *Int. J. Bifurcat. Chaos*, **29** (2019), 1930040. https://doi.org/10.1142/S0218127419300404
4. Q. Ouyang, *Introduction to Nonlinear Science and Pattern Dynamics*, 1st edition, Peking University Press, 2010.
5. J. Z. Cao, H. Sun, P. Hao, P. Wang, Bifurcation and turing instability for a predator-prey model with nonlinear reaction cross-diffusion, *Appl. Math. Model.*, **89** (2021), 1663–1677. https://doi.org/10.1016/j.apm.2020.08.030
6. H. Y. Sun, J. Cao, P. Wang, H. Jiang, Bifurcation and turing instability for genetic regulatory networks with diffusion, *Int. J. Biomath.*, (2022). https://doi.org/10.1142/S1793524522500711
7. H. G. Othmer, L. E. Scriven, Non-linear aspects of dynamic pattern in cellular networks, *J. Theor. Biol.*, **43** (1974), 83–112. https://doi.org/10.1016/S0022-5193(74)80047-0
8. H. Nakao, A. S. Mikhailov, Turing patterns in network-organized activator-inhibitor systems, *Nat. Phys.*, **6** (2010), 544–550. https://doi.org/10.1038/nphys1651
9. M. Asllani, J. D. Challenger, F. S. Pavone, L. Sacconi, D. Fanelli, The theory of pattern formation on directed networks, *Nat. Commun.*, **5** (2014), 4517. https://doi.org/10.1038/ncomms5517
10. S. Mimar, M. M. Juane, J. Park, A. P. Muñuzuri, G. Ghoshal Turing patterns mediated by network topology in homogeneous active systems, *Phys. Rev. E*, **99** (2019), 062303. https://doi.org/10.1103/PhysRevE.99.062303
11. Q. Zheng, J. Shen, Turing instability induced by random network in FitzHugh-Nagumo model, *Appl. Math. Comput.*, **381** (2020), 125304. https://doi.org/10.1016/j.amc.2020.125304
12. Q. Zheng, J. Shen, Y. Xu, Turing instability in the reaction-diffusion network, *Phys. Rev. E*, **102** (2020), 062215. https://doi.org/10.1103/PhysRevE.102.062215
13. Q. Zheng, J. Shen, Y. Xu, V. Pandey, L. Guanc, Pattern mechanism in stochastic SIR networks with ER connectivity, *Phys. A*, **603** (2022), 127765. https://doi.org/10.1016/j.physa.2022.127765
14. J. Ritchie, Turing instability and pattern formation on directed networks, preprint, arXiv: 2205.10946v1.
15. A. R. Kaye, W. S. Hart, J. Bromiley, S. Iwami, R. N. Thompson, A direct comparison of methods for assessing the threat from emerging infectious diseases in seasonally varying environments, *J. Theor. Biol.*, **548** (2022), 111195. https://doi.org/10.1016/j.jtbi.2022.111195
16. F. P. Agouanet, I. Tankam-Chedjou, R. M. Etoua, J. J. Tewa, Mathematical modelling of banana black sigatoka disease with delay and seasonality, *Appl. Math. Model*, **99** (2021), 380–399. https://doi.org/10.1016/j.apm.2021.06.030
17. V. P. Bajiya, J. P. Tripathi, V. Kakkar, J. Wang, G. Sun, Global dynamics of a multigroup SEIR epidemic model with infection age, *Chin. Ann. Math. B*, **42** (2021), 833–860. https://doi.org/10.1007/s11401-021-0294-1
18. R. Manjoo-Docrat, A spatio-stochastic model for the spread of infectious diseases, *J. Theor. Biol.*, **533** (2022), 110943. https://doi.org/10.1016/j.jtbi.2021.110943

19. G. Q. Sun, S. Wang, M. Li, L. Li, J. Zhang, W. Zhang, et al., Transmission dynamics of COVID-19 in Wuhan, China: Effects of lockdown and medical resources, *Nonlinear Dyn.*, **101** (2020), 1981–1993. https://doi.org/10.1007/s11071-020-05770-9
20. G. Q. Sun, M. Li, J. Zhang, W. Zhang, X. Pei, Z. Jin, Transmission dynamics of brucellosis: Mathematical modelling and applications in China, *Comput. Struct. Biotechnol. J.*, **18** (2020), 3843–3860. https://doi.org/10.1016/j.csbj.2020.11.014
21. X. Ma, X. Luo, L. Li, Y. Li, G. Sun, The influence of mask use on the spread of COVID-19 during pandemic in New York city, *Results Phys.*, **34** (2022), 105224. https://doi.org/10.1016/j.rinp.2022.105224
22. J. K. K. Asamoah, E. Okyere, A. Abidemi, S. E. Moore, G. Sun, Z. Jin, et al., Optimal control and comprehensive cost-effectiveness analysis for COVID-19, *Results Phys.*, **33** (2022), 105177. https://doi.org/10.1016/j.rinp.2022.105177
23. L. J. Pei, M. Y. Zhang, Long-term predictions of current confirmed and dead cases of COVID-19 in China by the non-autonomous delayed epidemic models, *Cogn. Neurodynamics*, **16** (2022), 229–238. https://doi.org/10.1007/s11571-021-09701-1
24. L. J. Pei, Prediction of numbers of the accumulative confirmed patients (NACP) and the plateau phase of 2019-nCoV in China, *Cogn. Neurodynamics*, **14** (2020), 411–424. https://doi.org/10.1007/s11571-020-09588-4
25. V. S. Rao, R. Durvasula, *Dynamic Models of Infectious Diseases*, New York, London, 2013. https://doi.org/10.1007/978-1-4614-3961-5
26. F. Brauer, C. Castillo-Chavez, Z. L. Feng, *Mathematical Models in Epidemiology*, Springer, New York, 2019. https://doi.org/10.1007/978-1-4939-9828-9
27. Y. Jin, W. D. Wang, S. W. Xiao, An SIRS model with a nonlinear incidence rate, *Chaos Solitons Fract.*, **34** (2007), 1482–1497. https://doi.org/10.1016/j.chaos.2006.04.022
28. Y. Y. Cai, Y. Kang, W. M. Wang, A stochastic SIRS epidemic model with nonlinear incidence rate, *Appl. Math. Comput.*, **305** (2017), 221–240. https://doi.org/10.1016/j.amc.2017.02.003
29. X. Y. Shi, Y. M. Cao, Dynamics of a stochastic periodic SIRS model with time delay, *Int. J. Biomath.*, **13** (2020), 2050072. https://doi.org/10.1142/S1793524520500722
30. I. Ali, S. U. Khan, Analysis of stochastic delayed SIRS model with exponential birth and saturated incidence rate, *Chaos Solitons Fract.*, **138** (2020), 110008. https://doi.org/10.1016/j.chaos.2020.110008
31. Q. Q. Zheng, V. Pandey, J. Shen, Y. Xu, L. Guan, Pattern dynamics in the epidemic model with diffusion network, *Europhys. Lett.*, **137** (2022), 42002.
32. D. Wang, Y. Zhao, J. Luo, H. Leng, Simplicial SIRS epidemic models with nonlinear incidence rates, *Chaos*, **31** (2021), 053112. https://doi.org/10.1063/5.0040518
33. W. J. Yang, Bifurcation and dynamics in double-delayed Chua circuits with periodic perturbation, *Chin. Phys. B*, **31** (2022), 020201. https://iopscience.iop.org/article/10.1088/1674-1056/ac1e0b
34. K. L. Cooke, Z. Grossman, Discrete delay, distributed delay and stability switches, *J. Math. Anal. Appl.*, **86** (1982), 592–627. https://doi.org/10.1016/0022-247X(82)90243-8

35. S. G. Ruan, Absolute stability, conditional stability and bifurcation in Kolmogorov-type predator-prey systems with discrete delays, *Quart. Appl. Math.*, **59** (2001), 159–173. https://doi.org/10.1090/qam/1811101

AIMS Press